Research Article

Meng-Zhen Zhou, Hao-Ran Wang, Xing Guo, Yan-Chan Wei, and Shuangquan Liao*

Synergistic effect of thermal oxygen and UV aging on natural rubber

https://doi.org/10.1515/epoly-2023-0016 received March 03, 2023; accepted April 26, 2023

Abstract: The oxidation of natural rubber (NR) leads to a decrease in mechanical properties, even resulting in failure of NR products. Many studies focusing on this single factor have failed to fully elucidate the impact of tropical island environment on NR properties. Based on this concern, the synergistic effect of thermal oxygen and ultraviolet (UV) aging on NR was systematically studied. The results revealed that thermal oxygenation can promote UV aging, which leads to the appearance of surface cracks and deepening of color. With the extension of aging time, the mechanical properties of NR correspondingly decreased. Besides, to deeply understand the mechanism of the synergistic effect of thermal oxygen and UV aging on NR, we selected squalene to simulate and analyze the molecular structure changes in NR. Based on these results, a possible synergistic effect of thermal oxygen and UV aging mechanisms on NR could be proposed.

Keywords: natural rubber, structure, thermal oxygen aging, UV aging, mechanical properties

1 Introduction

Natural rubber (NR) has received great attention in various industries (1–4) owing to its unique elasticity, high tear strength, and excellent flexibility (5,6). The comprehensive performance of NR as a general elastomer material is better than that of synthetic rubber (7,8). The non-rubber components in NR, mainly proteins and phospholipids, are

believed to be the reason why it has better comprehensive performance than synthetic rubber (9,10). So, NR and NR nanocomposites are more widely used in engineering materials (11). Engineering materials often face more stringent external environments, e.g., tropical island environment, including heat (12), oxygen (13), and ultraviolet (UV) radiation (14). However, NR has unstable double bonds, which are prone to degrade (15). NR may encounter declined physical properties and even shortened service life.

The study of thermal oxygen aging of NR has always been a hot spot in the industry. When NR is exposed to the thermal oxidative environment, polysulfide bonds are dissociated by heating to form monosulfide and disulfide bonds (16–18). In the process of thermal oxygenation, NR oxidized and degraded to produce carbon radicals R. which combine with oxygen to form ROO. The hydrogen atoms on the NR chain are trapped and converted into a more active ROO, resulting in R. (19). The degradation of NR produces oxygen-containing functional groups, which eventually lead to chain fracture (20). Oxidation and chain breakage of bonds have negative effects on NR performance. However, the application of heating alone is not representative of the tropical island environment, including UV irradiation, which promotes oxidation processes and leads to the aging of NR (21). UV irradiation can attack double bonds to produce unstable peroxy radicals in the presence of oxygen (22). UV irradiation of NR eventually induces various oxidation products such as ketones, aldehydes, and organic acids (15,23). Both heat and UV irradiation can degrade the properties of NR, but their effects on NR aging are different (24). A more complicated aging behavior is observed when heat and UV radiation are combined. However, the existing research mainly focuses on a single aging factor, which cannot provide the most accurate service life prediction for the actual use of NR. The service life of rubber products that are designed according to a single aging factor cannot fully represent the actual service life, which inevitably leads to premature failure of the products (25,26). Based on this, Li et al. (27) observed the silicone rubber degradation process in two test conditions prepared according

^{*} Corresponding author: Shuangquan Liao, Natural Rubber Cooperative Innovation Center of Hainan Province and Ministry of Education of China, School of Materials Science and Engineering, Hainan University, Haikou, China, e-mail: lsqhnu@hainanu.edu.cn Meng-Zhen Zhou, Hao-Ran Wang, Xing Guo, Yan-Chan Wei: Natural Rubber Cooperative Innovation Center of Hainan Province and Ministry of Education of China, School of Materials Science and Engineering, Hainan University, Haikou, China

to real proton exchange membrane fuel cell operational conditions and analyzed the degradation mechanisms. The relation between time and concentration can be constructed to predict the lifetime of the material according to the time-temperature superposition principle. Li et al. (28) proposed a novel accelerated aging test method based on the dominant damage mechanism of rubber material caused by temperature cycle treatments. Based on this method, the long-term aging test results of rubber samples under high- and low-temperature cycle conditions can be predicted. Yang et al. (29) applied three different approaches to investigate the fatigue life of the styrene-butadiene rubber vulcanizates and established a fatigue life prediction model based on strain amplitude as the damage parameter. Understanding the thermal oxygen and UV aging synergistic mechanisms on NR, herein, is rather significant for the NR industry.

In this work, combining thermal oxygen with UV aging was performed on a dumbbell NR sample in the UV aging chamber for different aging times. The changes of molecular structure of NR before and after aging were studied by Fourier transform infrared spectroscopy (FTIR) and Raman spectroscopy. The aging degree is expressed by comparing the macroscopic mechanical properties of NR under different aging conditions. Besides, to deeply understand the mechanism of the synergistic effect of thermal oxygen and UV aging, we selected squalene to simulate and analyze the molecular structure changes in NR. The current study aims to investigate the synergistic effect of thermal oxygen and UV aging on NR. This study of aging can provide theoretical guidance on understanding the anti-aging properties of rubber products (30), as well as a data basis for product life prediction (31) and a safety guarantee for the safe use of products.

2 Experimental

2.1 Materials

NR was provided by China Hainan Rubber Industry Group Co., Ltd. Zinc oxide analytical purity of the reagent (AR), sulfur (AR), analytical purity of the reagent (AR), stearic acid (AR), and 2-mercaptobenzothiazole (AR) were obtained from Shanghai Aladdin Bio-Chem Technology Co., Ltd.

2.2 Samples preparation

About 100 phr NR were mixed via a two-roll mill, and then 3 phr sulfur, 5 phr ZnO, 0.5 phr stearic acid, and

0.7 phr 2-mercaptobenzothiazole were added to the NR on the two-roll mill at room temperature. After complete mixing, the compounds were compressed at 145°C, and the optimum curing time was determined by a vulcameter.

2.3 Aging process

UV aging tests were carried out in the HDUVA-340 UV aging chamber. UV-A radiation (315-400 nm) accounts for approximately 95% of the UV radiation reaching the Earth's surface (32). The UV source consisted of a UV-A-340 lamp, which produced peek emission at 340 nm and UV-A irradiation with a UV intensity of 1.35 W⋅m⁻². The NR samples were exposed to UV radiation for 24, 48, 72, 96, and 120 h at 40°C. Thermal oxygen aging tests were carried out in the HDUVA-340 UV aging chamber. The NR samples were exposed to 80°C for 24, 48, 72, 96, and 120 h. Synergistic effect of thermal oxygen and UV aging tests were carried out in the HDUVA-340 UV aging chamber. The NR samples were exposed to 80°C for 24, 48, 72, 96, and 120 h. Synergistic effect of thermal oxygen and UV aging tests were carried out in the HDUVA-340 UV aging chamber. The NR samples were exposed to UV radiation for 24, 48, 72, 96, and 120 h at 80°C.

2.4 Characterizations

2.4.1 Scanning electron microscopy (SEM)

To compare the surface change before and after aging, microtopography imaging of specimens was performed using the S-4800 SEM at $1,000 \times$ magnifications with an applied voltage of 5 kV. Since NR is the insulating material, samples with different aging times were coated with a gold layer.

2.4.2 FTIR spectrometer

FTIR spectra were recorded on a Nicolet iS50 + Nicolet continuum FTIR spectrometer at room temperature. The wavenumber range was from 4,000 to 400 cm⁻¹ with 16 scans. FTIR spectra could be used to obtain detailed information about the functional groups on the NR before and after aging.

2.4.3 Raman spectroscopy

Raman spectra were recorded on the inVia Qontor Raman spectrometer at room temperature. Raman spectra of the unaging NR samples were illuminated with a He–Ne laser

source, selecting the red line at 785 nm. Raman spectra of the aging NR samples were illuminated with a He-Cd laser source selecting the UV at 325 nm. The Raman shift range was selected between 100 and 3,000 cm⁻¹ with three accumulations and each acquisition time of 10 s.

2.4.4 Cross-linking density

Vulcanized NR samples of about 0.2 g (m_1) were soaked in toluene at room temperature for 7 days, and the solvent was then rapidly removed from the swollen sample surface by filter paper. The swollen samples were weighed (m_2) . Cross-linking density calculated according to the classical Flory-Rehner equation (33):

$$\varphi_r = \frac{m_1/\rho + m_2/\rho_s}{m_1/\rho} \tag{1}$$

$$-\ln(1-\varphi_r) - \varphi_r - \chi_r \varphi_r^2 = nV_0(\varphi_r^{\frac{1}{3}} - \frac{1}{2}\varphi_r)$$
 (2)

$$M_c = \frac{\rho}{n} \tag{3}$$

where φ_r is the volume fraction of polymer in the swollen network, V_0 is the molar volume of the solvent (106.2 mL·mol⁻¹ for toluene), χ_r is the Flory–Huggins polymer–solvent interaction term (0.393 for NR/toluene), n is the average number of movable chain segments per unit volume (mol·mL⁻¹), M_c is the average mass of network chains, ρ is the density of NR (0.913 g·mL $^{-1}$ for NR), and $\rho_{\rm s}$ is the density of toluene $(0.866 \text{ g} \cdot \text{mL}^{-1}).$

2.4.5 ¹H nuclear magnetic resonance (NMR) spectroscopy

The 500 µL squalene and 500 µL CDCl₃ were mixed into a 5 mm test tube for NMR. NMR spectra were acquired on Avance 400 MHz Bruker NMR spectrometer. ¹H NMR spectra were acquired by 16 accumulations and each acquisition time of 4 s.

2.4.6 Mechanical properties measurements

The mechanical property was performed on dumbbellshaped samples (75 mm \times 4 mm \times 1 mm and a test length of 20 mm) by a Gotech AI-3000 universal testing machine. The measurement was performed at room temperature with a speed of 500 mm·min⁻¹. In this study, three specimens of each sample were measured for the tensile tests to evaluate the aging degree of NR.

Results and discussion

3.1 Synergistic effect of thermal oxygen and UV aging on the surface of NR

As shown in Figure 1, the initial NR surface was smooth. Some mild cracks appeared on the surface of NR, and the color of the NR surface slightly deepened after 48 h of UV aging. Nevertheless, the surface of NR remained smooth, and the color of the NR surface has not been changed after thermal oxygen aging. Some cracks occurred on the NRsurface and the color of the NR surfaceobyiously deepened after 24 hsynergistic effect of thermal oxygen andUV aging. As time went by, the cracks became more obvious, and the color of the NR surface became darker. Under UV irradiation, when the temperature increased from 40°C to 80°C, the cracks appeared earlier, and the cracks became more obvious. The SEM images are shown in Figure 2. The surfaces of the NR became porous and

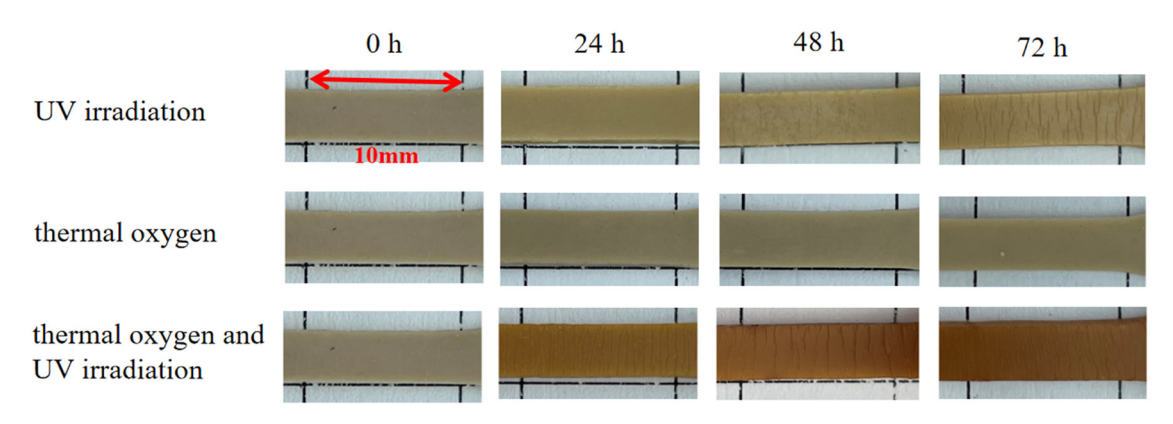


Figure 1: Surface morphology changes of NR under different aging conditions.

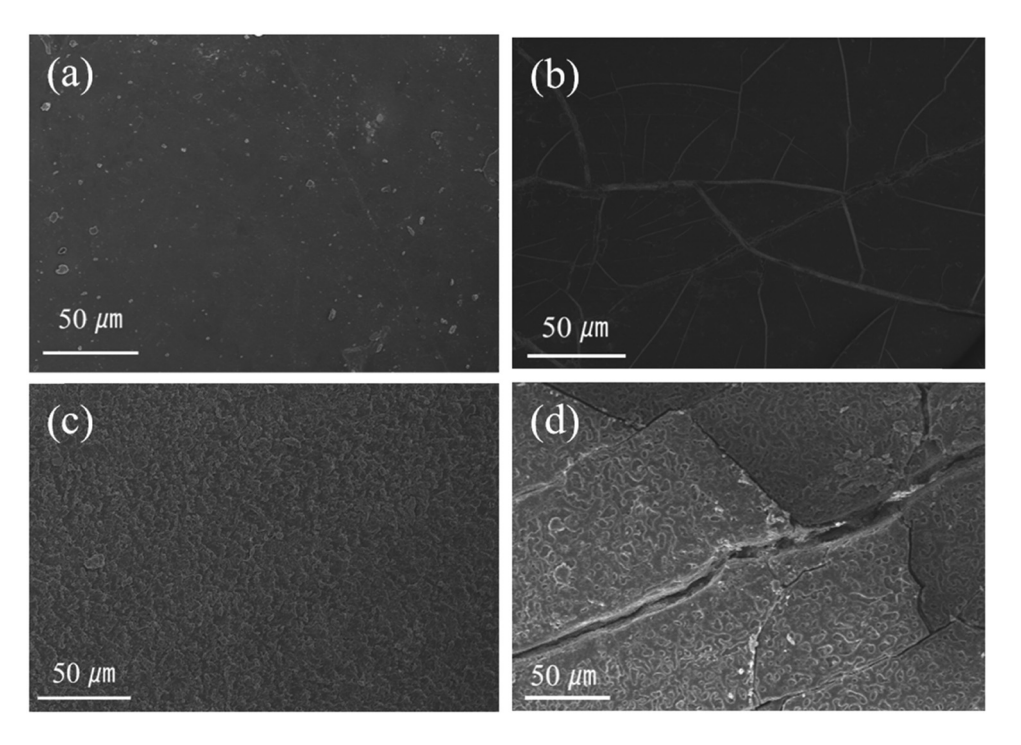


Figure 2: SEM images of NR with 48 h aging under different aging conditions: (a) pristine, (b) UV irradiation (exposed to 40° C and UV irradiation with an intensity of 1.35 W·m⁻²), (c) thermal oxygen (exposed to 80° C), (d) combine effect of thermal oxygen and UV irradiation (exposed to 80° C and UV irradiation with intensity of 1.35 W·m⁻²).

rough after 48 h of thermal oxygen aging. This phenomenon was mainly attributed to small molecules escaping from the NR surface and generating some degraded small molecules. But no cracks appeared. Therefore, UV irradiation is the main cause of cracks of NR.

Meanwhile, these obtained results demonstrated that the synergistic effect of thermal oxygen and UV on the NR aging process was a continuous destruction process from the surface to the interior. UV irradiation caused cracks and color deepening on the surface of NR. In addition, the temperature played an important role in the synergistic effect of thermal oxygen and UV aging process.

3.2 Synergistic effect of thermal oxygen and UV aging on mechanical properties of NR

The mechanical properties of NR at different aging conditions were further investigated. The tensile strength and elongation at the break of samples show a downward trend with increasing aging time (Figure 3). Before aging, the tensile strength and elongation at break were 20.97 MPa and 825.30%. After 120 h of UV aging, the retention of tensile strength and retention of elongation at the break for NR decreased to 53.48% (11.21 MPa) and 93.22% (769.33%). After 120 h of thermal oxygen aging, the retention of tensile

strength and retention of elongation at the break for NR decreased to 57.09% (11.97 MPa) and 77.18% (636.93%). After 120 h, the synergistic effect of thermal oxygen and UV aging, the retention of tensile strength, and the retention of elongation at the break for NR decreased to 32.45% (6.80 MPa) and 65.68% (542.03%). As shown in Figure 3, the tensile strength retention rate and the elongation at break retention rate of aging NR decreased with aging time, which demonstrated that the mechanical properties can decrease with aging time. Figure 3 shows that the elongation at break is very sensitive to thermal oxygen aging, and the tensile strength is very sensitive to UV aging. In addition, it was found that the retention of tensile strength and retention of elongation at break of NR after the synergistic effect of thermal oxygen and UV aging was slightly lower than the other two kinds of aging NR, suggesting that the thermal oxygen and UV irradiation intensity of the NR aging process have the function of mutual promotion.

3.3 Synergistic effect of thermal oxygen and UV aging on the molecular structure of NR

In order to monitor the change of NR functional groups after UV irradiation, attenuated total reflection Fourier

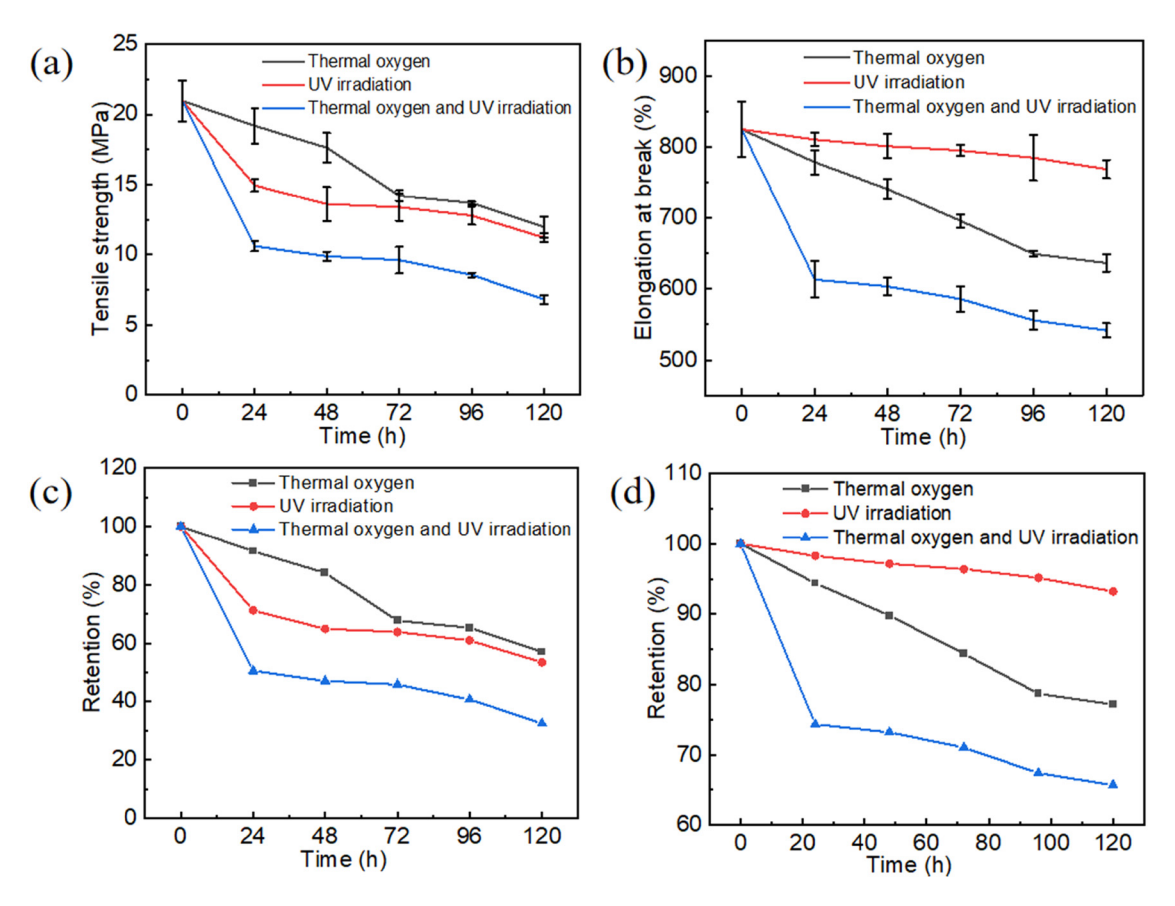


Figure 3: (a) Tensile strength of NR under different aging conditions. (b) Elongation at break of NR under the different aging conditions. (c) The tensile strength retention rate of NR under different aging conditions. (d) Elongation at break retention rate of NR under different aging conditions.

transform infrared spectroscopy (ATR-FTIR) was used. Figure 4a shows ATR-FTIR spectra of the NR before and after UV aging. Before aging, the NR exhibited absorption bands at 837 cm⁻¹, which is assigned to C=C-H out-ofplane deformation (34). The absorption bands at 1,375 and 1,452 cm⁻¹ can be assigned to -CH₃ and -CH₂ deformations, respectively. The absorption bands of -CH₂ symmetric, -CH₂ asymmetric, and -CH₃ asymmetric stretching can be observed at 2,850, 2,918, and 2,960 cm⁻¹, respectively (35,36). After UV aging, the characteristic absorption bands at 837 cm⁻¹ decreased in intensity, indicating that the C=C of NR was partially destroyed during the UV aging process. In addition, some new peaks can be observed, and the strong peaks at 1,645 and 1,707 cm⁻¹ are assigned to C=O stretching vibration, which means the formation of carbonyl groups and aldehyde groups. The peak at 1,080 cm⁻¹ is assigned to C-O-C asymmetric stretching, which means the formation of ether bonds due to the photo-oxidation at the main NR chain. The peak at 3,300 cm⁻¹ is assigned to O-H asymmetric stretching (37). The photo-oxidation reaction led to chain scission of NR and generated various oxidized

products (14), such as carbonyl groups, aldehyde groups, ether bonds, and hydroxyl groups.

As shown in Figure 4b, after thermal oxygen aging, the characteristic absorption bands at 837 cm⁻¹ decreased in intensity, indicating that the C=C of NR was partially destroyed during the thermal oxygen aging process. Some new peaks can be observed; the strong peak at 1,645 cm⁻¹ is assigned to C=O stretching vibration, which means the formation of carbonyl groups and aldehyde groups due to the thermal oxidation destroyed the main NR chain. It indicates that both thermal oxygen aging and photo-oxidation aging attack the C=C of NR and generate carbonyl groups, aldehyde groups, and hydroxyl groups.

By comparing Figure 4a and c, we observe that when the UV aging temperature increases from 40°C to 80°C, the intensity of functional groups corresponding to the oxidation products increases. These proved that high temperature can promote UV aging. Figure 4c shows ATR-FTIR spectra of the NR before and after the combine effect of thermal oxygen and UV aging. After the combine effect of thermal oxygen and UV irradiation, the characteristic

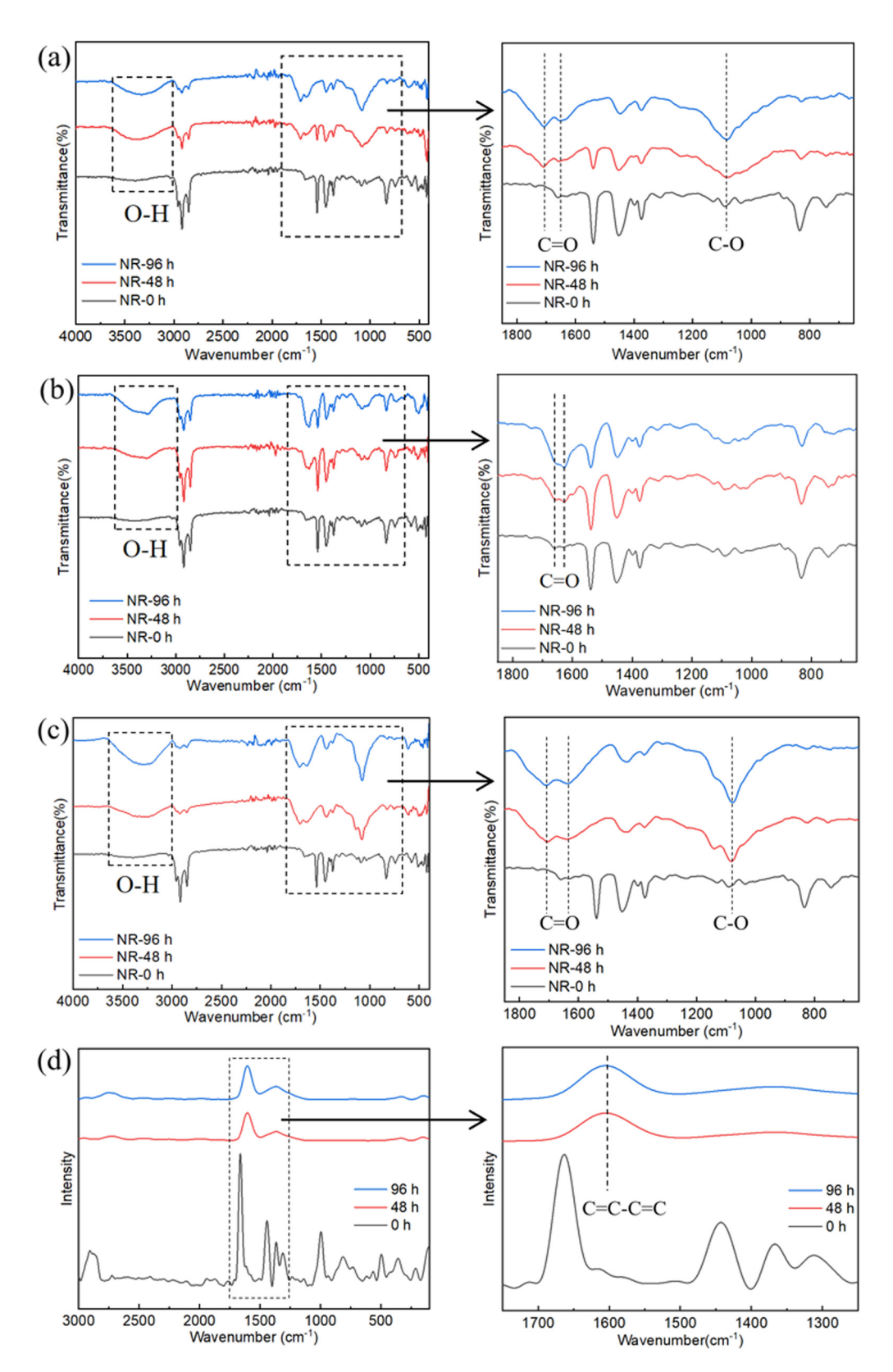


Figure 4: (a) FTIR spectra of NR at UV irradiation (exposed to 40°C and UV irradiation with an intensity of 1.35 W·m⁻²). (b) FTIR spectra of NR at thermal oxygen (exposed to 80°C). (c) FTIR spectra of NR at combine effect of thermal oxygen and UV irradiation (exposed to 80°C and UV irradiation with intensity of 1.35 W·m⁻²). (d) Raman spectra of NR at combine effect of thermal oxygen and UV irradiation.

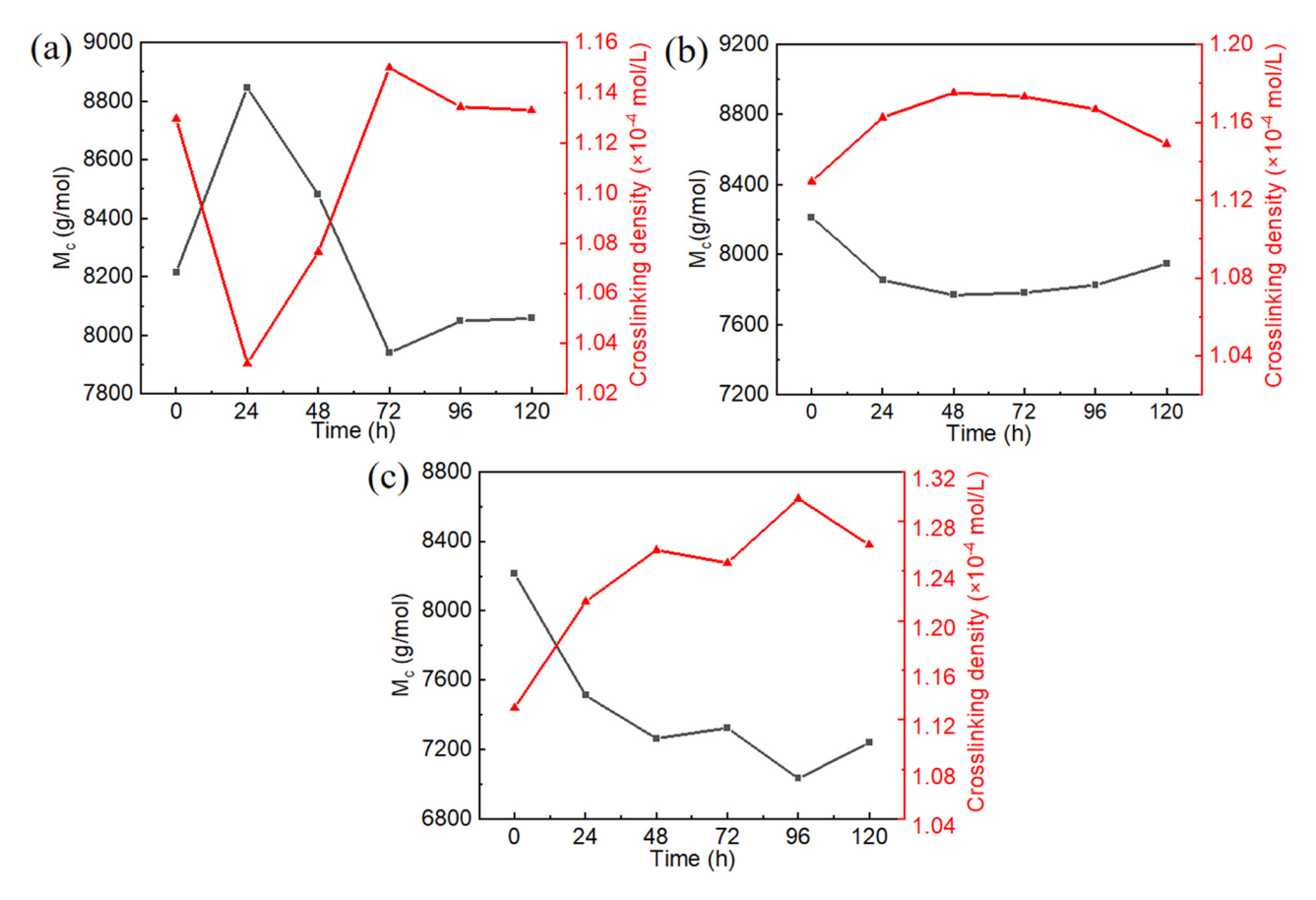


Figure 5: Cross-link density and M_c of NR by different aging conditions: (a) UV irradiation (exposed to 40°C and UV radiation with an intensity of 1.35 W·m⁻²), (b) thermal oxygen (exposed to 80°C), (c) thermal oxygen and UV irradiation (exposed to 80°C and UV radiation with an intensity of 1.35 W·m⁻²).

absorption bands at 837 cm⁻¹ decreased in intensity, indicating that the C=C of NR was partially destroyed. In addition, some new peaks can be observed; the strong peaks at 1,645 and 1,707 cm⁻¹ are assigned to C=O stretching vibration, which means the formation of carbonyl groups and aldehyde groups. The peak at 1,080 cm⁻¹ is assigned to C-O-C asymmetric stretching, which means the formation of ether bonds due to the photo-oxidation at the main NR chain. The peak at 3,300 cm⁻¹ is assigned to O-H asymmetric stretching. Figure 4d shows the Raman spectra of the NR before and after the combine effect of thermal oxygen and UV aging. The characteristic absorption bands at 1,665 cm⁻¹ of C=C stretching of *cis*-polyisoprene chain and 2,900 cm⁻¹ of C-H stretching decreased in intensity (38,39). After the combine effect of thermal oxygen and UV irradiation, the characteristic absorption bands at 1,665 cm⁻¹ decreased in intensity, indicating that the C=C of NR was partially destroyed during the thermal oxygen and UV aging processes. The strong peaks at 1,600 cm⁻¹ can be observed, which means the formation of C=C-C=C during the thermal oxygen and UV aging process (40,41). According to these results, NR can be protected from

thermal oxygen and UV aging by the Diels-Alder diene synthesis reaction of conjugated double bonds.

3.4 Synergistic effect of thermal oxygen and UV aging on cross-link density of NR

The vulcanized NR forms a three-dimensional cross-linking network between the rubber molecular chains, and the cross-linking degree can be expressed by the cross-linking density or the average molecular weight (M_c) between the cross-linking points. As shown in Figure 5a, during the UV aging process, the M_c was decreased initially and increased at a later stage. On the contrary, the cross-link density was increased initially and decreased at a later stage. The cross-link densities of NR were 1.13×10^{-4} and 1.03×10^{-4} mol·mL⁻¹ before and after initial 24 h UV aging, respectively, which displayed an 8.85% difference. The chain-scission reaction played the dominant role, bringing about the reduction of cross-linking density. The UV irradiation process of NR fractures molecular bonds and cross-linking bonds, bringing

about the reduction of cross-linking density. The UV irradiation process of NR fractures C–H and C=C bonds, which produce carbon radicals R·. The UV irradiation process of NR fractures cross-linking bonds, which produces free sulfur content. The cross-link density of NR was $1.13 \times 10^{-4} \, \text{mol-mL}^{-1}$ after 120 h UV aging, which decreased by 8.85%. The increase in cross-link density generally results from the cross-linking reaction of free sulfur content and carbon radicals R·, which leads to the post-curing process during the aging period (42). These phenomena indicated that NR was in the state of chain scission and cross-linking during UV aging, and its cross-linking density ultimately tended to increase. It means that the cross-linking reaction is dominant during UV aging.

As shown in Figure 5b, during the thermal oxygen aging process, the cross-link density was increased initially and decreased at a later stage. The cross-link densities of NR were 1.13×10^{-4} and 1.18×10^{-4} mol·mL⁻¹ before and after the initial 48 h thermal oxygen aging, respectively, which displayed a 4.42% difference. The cross-link density of NR was 1.15×10^{-4} mol·mL⁻¹ after 120 h thermal oxygen aging, which decreased by 2.54%. Thermal oxygen aging in NR is known to be a stepwise process. The initial increase is due to the degradation of unstable polysulfide to mono- and disulfide. The decrease in the cross-link density after 48 h is due to the further decomposition of mono-, di-, and polysulfide (17).

The cross-link densities of NR before and after the combine effect of thermal oxygen and UV irradiation are shown in Figure 5a. As the aging time went by, the cross-link density of NR did not remain at a stable level; however, it showed an overall trend of increasing. The cross-link density increased initially and decreased at a later stage. The cross-link density of NR increased after the initial 96 h combine effect of thermal oxygen and UV irradiation. The cross-link densities of NR were 1.13×10^{-4} and $1.30 \times 10^{-4} \, \text{mol} \cdot \text{mL}^{-1}$ before and after 96 h under the combine effect of thermal oxygen and UV irradiation, respectively, which increased 15.04%. The increase in cross-link density generally results from the cross-linking reaction of free sulfur content and carbon radicals R. which leads to post-curing process during the aging period. In addition, it is due to the degradation of unstable polysulfide to mono- and disulfide. Compared with UV aging, the increase in temperature promoted the crosslinking reaction of free sulfur content and carbon radicals R, resulting in an increase in the cross-linking density of NR after the initial 96 h combine effect of thermal oxygen and UV irradiation. The cross-link densities of NR were 1.30×10^{-4} and $1.26 \times 10^{-4} \, \text{mol} \cdot \text{mL}^{-1}$ before and after 96 h under the combine effect of thermal oxygen and UV

irradiation, respectively, which decreased 0.032%. The decrease in the cross-link density after 96 h is due to the further decomposition of mono-, di-, and polysulfide. The cross-link density of NR after the combine effect of thermal oxygen and UV irradiation decreased first may be due to the promotion of temperature to UV aging. Therefore, the cross-linking reaction tended to dominate this process.

3.5 Synergistic effect of thermal oxygen and UV on NR aging degradation mechanism

To have a deeper understanding of the mechanism of the synergistic effect of thermal oxygen and UV aging on NR, we selected squalene, a small molecule with a similar structure to NR, to analyze the molecular structure changes of NR and simulate the synergistic effect of thermal oxygen and UV aging process of NR. Figure 6a shows the FTIR spectra of the squalene before and after the combine effect of thermal oxygen and UV aging. Before aging, the squalene exhibited absorption bands at 837 cm⁻¹, which is assigned to C=C-H out-of-plane deformation. The absorption bands at 1,375 and 1,452 cm⁻¹ can be assigned to -CH₃ and -CH₂ deformations, respectively. The absorption bands of -CH₂ symmetric, -CH₂ asymmetric, and -CH₃ asymmetric stretching can be observed at 2,850, 2,918, and 2,960 cm⁻¹, respectively. The typical characteristic peak C-H of C=C-H at 837 cm⁻¹ and typical characteristic peak C=C at 1,660 cm⁻¹ for squalene gradually disappeared with increasing aging time (Figure 6a). Besides, some new peaks appeared at 1,730 and 1,073 cm⁻¹, respectively, indicating that the double bonds in squalene were destroyed by heat and UV radiation along with the formation of C=O and C-O-C (43.44). Furthermore, the aging products of squalene after the synergistic effect of thermal oxygen and UV aging were confirmed by ¹H NMR analysis (Figure 6b). This suggests that the occurrence of photochemical reactions may involve the generation of allylic radicals (45). The ¹H NMR of squalene after synergistic effect of thermal oxygen and UV aging indicated that the generation of non-allylic CH₂/CH₃ signals at 1.2 ppm (46). This is compelling evidence that double bonds are lost in this photochemically driven process.

The macroscopic and microscopic properties of NR materials are decreased by the synergistic effect of thermal oxygen and UV aging, and complex bond breaking, crosslinking, and oxidation reactions occur on the surface of materials. For NR, the reaction as shown in Figure 6c may occur when it suffers from the combine effect of thermal oxygen and UV irradiation. The heating and UV irradiation processes of NR fracture the C–H bonds of methylene and

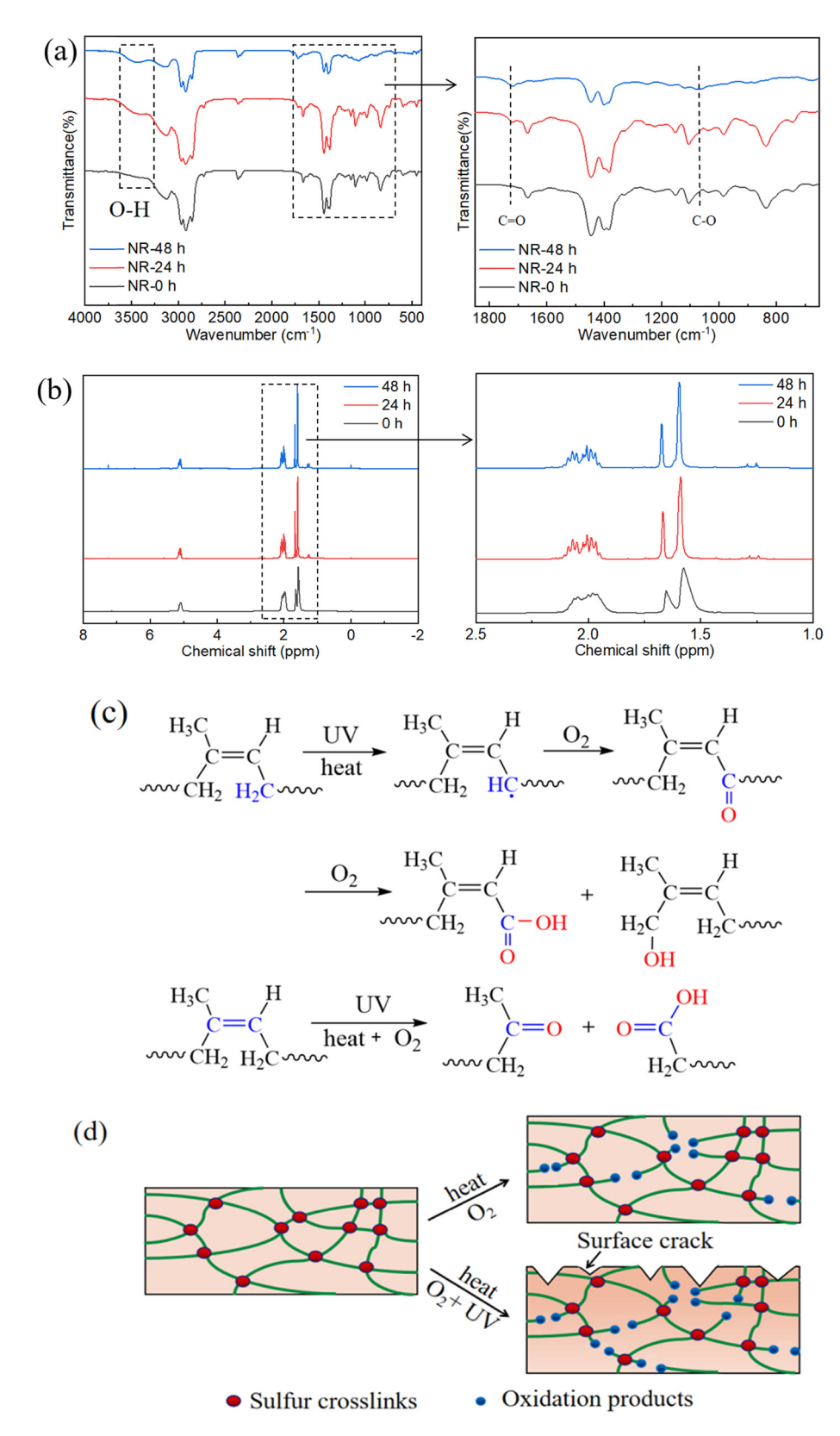


Figure 6: FTIR (a) and ¹H NMR (b) spectra of squalene before and after reacting with combine effect of thermal oxygen and UV irradiation. (c) Schematic diagram of the potential mechanism for the synergistic effect of thermal oxygen and UV on NR aging. (d) A schematic diagram of the changes of cross-linking network structure for NR after aging.

produce carbon radicals R, which combine with oxygen to produce aldehyde groups. The further oxidation of NR forms oxygen-containing functional groups such as carboxyl groups and hydroxyl groups, which eventually lead to chain fracture. The heating and UV irradiation process of NR fractures the C=C bonds. The further oxidation of NR forms oxygen-containing functional groups such as carbonyl groups and carboxyl groups, which eventually lead to chain fracture. The C-H bonds of methylene and C=C bonds in the NR are oxidized, which increases O-H bonds and C=O bonds in the molecule, while the content of C-H and C=C bonds decrease. In addition, the bond energies of C-H of $-CH_3$, C-H of $-CH_2$, and C=C are 351.6, 335.7, and 271.63 kJ·mol⁻¹, respectively, which are all less than the energy of the UV-A ultraviolet photon that is 352 kJ·mol⁻¹ (47). Thus, C-H and C=C bonds in NR molecules fracture to a certain extent, resulting in material deterioration. We come up with the potential aging process, which is shown in Figure 6d. The heating process of NR fractures the C-H bonds and C=C bonds, causing chain breakage that produces various oxidation products. Compared with thermal oxygen aging, the surface of NR appeared cracked; the color of the NR surface obviously deepened and broke more bonds after the synergistic effect of thermal oxygen and

4 Conclusion

UV aging.

10

In this study, the synergistic effect of thermal oxygen and UV aging on NR was studied. The results show that the surface morphology, molecular structure, and mechanical properties of NR changed dramatically during the combine effect of thermal oxygen and UV irradiation. It is worth noting that thermal can promote UV aging, which leads to the appearance of surface cracks and deepening of color. The synergistic effect of thermal oxygen and UV aging of NR is a process from the surface to the inside. During this period, the size of cracks gradually increased with the aging time. With the extension of aging time, the mechanical properties of NR, such as tensile strength and elongation at break, were correspondingly reduced since the molecular chain network structures and cross-linking points of NR were destroyed. The simulated aging process of NR by squalene proved that heat and UV can destroy C=C and C-H in the molecular chain of olefins and form alkyl aldehydes, ketones, aliphatic esters, and ether compounds. Based on these results, a synergistic mechanism of thermal oxygen and UV aging on NR was proposed.

Funding information: This research was supported by the Hainan Provincial Joint Project of Sanya Yazhou Bay Science and Technology City (Grant No. 520LH023), the Key-Area Research and Development Program of Guangdong Province (No. 2020B020217003), and the Hainan Provincial Natural Science Foundation (No. 521CXTD438).

Author contributions: Meng-Zhen Zhou: writing – original draft, investigation, writing – review and editing, methodology, experiment, data analysis and plotting; Hao-Ran Wang: experiment, data analysis and plotting; Xing Guo: investigation, writing – review and editing; Yan-Chan Wei: methodology, data analysis, writing – review and editing; Shuangquan Liao: writing – review and editing, resources.

Conflict of interest: The authors state that there is no conflict of interest.

Data availability statement: The data sets generated and/ or analyzed during the current study are available from the corresponding author on reasonable request.

References

- (1) Guerra NB, Sant'Ana Pegorin G, Boratto MH, de Barros NR, de Oliveira Graeff CF, Herculano RD. Biomedical applications of natural rubber latex from the rubber tree *Hevea brasiliensis*. Mater Sci Eng C. 2021;126:112126–43. doi: 10.1016/j.msec. 2021.112126.
- (2) Fu X, Xie Z, Wei L, Huang C, Luo M, Huang G. Detecting structural orientation in isoprene rubber/multiwall carbon nanotube nanocomposites at different scales during uniaxial deformation. Polym Int. 2018;67:258–68. doi: 10.1002/pi.5491.
- (3) Ansari AH, Jakarni FM, Muniandy R, Hassim S, Elahi Z. Natural rubber as a renewable and sustainable bio-modifier for pavement applications: A review. J Clean Prod. 2021;289:125727-42. doi: 10.1016/j.jclepro.2020.125727.
- (4) Duan X, Cheng S, Tao R, Zhang Z, Zhao G. Synergistically enhanced thermal control ability and mechanical properties of natural rubber for tires through a graphene/silica with a dotface structure. Adv Compos Hybrid Mater. 2022;5:1145–57. doi: 10.1007/s42114-022-00453-y.
- (5) Zhou Y, Kosugi K, Yamamoto Y, Kawahara S. Effect of nonrubber components on the mechanical properties of natural rubber. Polym Adv Technol. 2017;28:159–65. doi: 10.1002/ pat.3870.
- (6) Sebald G, Xie Z, Guyomar D. Fatigue effect of elastocaloric properties in natural rubber. Philos Trans A Math Phys Eng Sci. 2016;374:2074–86. doi: 10.1098/rsta.2015.0302.
- (7) Bennacer R, Liu B, Yang M, Chen A. Refrigeration performance and the elastocaloric effect in natural and synthetic rubbers.

- Appl Therm Eng. 2022;204:117938. doi: 10.1016/j. applthermaleng.2021.117938.
- (8) Soratana K, Rasutis D, Azarabadi H, Eranki PL, Landis AE. Guayule as an alternative source of natural rubber: A comparative life cycle assessment with Hevea and synthetic rubber. J Clean Prod. 2017;159:271-80. doi: 10.1016/j.jclepro.2017.05.070.
- Huang C, Zhang J, Cai X, Huang G, Wu J. The effects of proteins and phospholipids on the network structure of natural rubber: a rheological study in bulk and in solution. J Polym Res. 2020;27:158-68. doi: 10.1007/s10965-020-02147-9.
- (10) Huang C, Huang G, Li S, Luo M, Liu H, Fu X, et al. Research on architecture and composition of natural network in natural rubber. Polymer. 2018;154:90-100. doi: 10.1016/j.polymer. 2018.08.057.
- (11) Li H, Yang L, Weng G, Xing W, Wu J, Huang G. Toughening rubbers with a hybrid filler network of graphene and carbon nanotubes. J Mater Chem A. 2015;3:22385-92. doi: 10.1039/ c5ta05836h.
- (12) Zhang Z, Sun J, Lai Y, Wang Y, Liu X, Shi S, et al. Effects of thermal aging on uniaxial ratcheting behavior of vulcanised natural rubber. Polym Test. 2018;70:102-10. doi: 10.1016/j. polymertesting.2018.06.030.
- (13) Wei Y-C, Xie W-Y, He M-F, Zhu D, Liu S, Zhang L, et al. The role of non-rubber components acting as endogenous antioxidants on thermal-oxidative aging behavior of natural rubber. Polym Test. 2022;111:107614. doi: 10.1016/j.polymertesting.2022. 107614.
- (14) Tertyshnaya Y, Podzorova M, Moskovskiy M. Impact of water and UV irradiation on nonwoven polylactide/natural rubber fiber. Polymers. 2021;13:461-70. doi: 10. 3390/ polym13030461.
- (15) Tasakorn P, Amatyakul W. Photochemical reduction of molecular weight and number of double bonds in natural rubber film. Korean J Chem Eng. 2008;25:1532-8. doi: 10.1007/ s11814-008-0252-6.
- (16) Jiang Y, Zhang Y. Improving thermal oxidative aging resistance and anti-reversion property of natural rubber by adding a crosslinking agent. J Appl Polym Sci. 2021;139:51882. doi: 10. 1002/app.51882.
- (17) Lee YH, Cho M, Nam JD, Lee YK. Effect of ZnO particle sizes on thermal aging behavior of natural rubber vulcanizates. Polym Degrad Stab. 2018;148:50-5. doi: 10.1016/j.polymdegradstab. 2018.01.004.
- (18) Fan R, Zhang Y, Huang C, Zhang Y, Fan Y, Sun K. Effect of crosslink structures on dynamic mechanical properties of natural rubber vulcanizates under different aging conditions. J Appl Polym Sci. 2001;81:710-8. doi: 10.1002/app.1488.
- (19) Wang M, Wang R, Chen X, Kong Y, Huang Y, Lv Y, et al. Effect of non-rubber components on the crosslinking structure and thermo-oxidative degradation of natural rubber. Polym Degrad Stab. 2022;196:109845. doi: 10.1016/j.polymdegradstab. 2022.109845.
- (20) Chaikumpollert O, Sae-Heng K, Wakisaka O, Mase A, Yamamoto Y, Kawahara S. Low temperature degradation and characterization of natural rubber. Polym Degrad Stab. 2011;96:1989-95. doi: 10.1016/j.polymdegradstab.2011.
- (21) Murakami K, Takasugi S. Chemorheological studies on polymer degradation. J Appl Polym Sci. 1977;21:55-63. doi: 10.1002/app.1977.070210105.

- (22) Rooshenass P, Yahya R, Gan SN. Preparation of liquid epoxidized natural rubber by oxidative degradations using periodic acid, potassium permanganate and UV-irradiation. J Polym Environ. 2017;26:1378-92. doi: 10.1007/s10924-017-1038-x.
- (23) Seentrakoon B, Junhasavasdikul B, Chavasiri W. Enhanced UVprotection and antibacterial properties of natural rubber/ rutile-TiO2 nanocomposites. Polym Degrad Stab. 2013;98:566-78. doi: 10.1016/j.polymdegradstab.2012.
- (24) Bhowmick AK, White JR. UV- and sunlight ageing of thermoplastic elastomeric natural rubber-polyethylene blends. J Mater Sci. 2002;37:5141-51. doi: 10.1023/A:1021076724403.
- (25) Su C, Pan A-X, Gong Y, Yang Z-G. Failure analysis on rubber universal spherical joints for rail vehicles. Eng Fail Anal. 2021;126:105453. doi: 10.1016/j.engfailanal.2021.105453.
- (26) Fedorko G, Molnár V, Michalik P, Dovica M, Tóth T, Kelemenová T. Extension of inner structures of textile rubber conveyor belt - Failure analysis. Eng Fail Anal. 2016;70:22-30. doi: 10.1016/j.engfailanal.2016.07.006.
- (27) Li G, Zhu D, Jia W, Zhang F. Analysis of the aging mechanism and life evaluation of elastomers in simulated proton exchange membrane fuel cell environments. e-Polymers. 2021;21:921-9. doi: 10.1515/epoly-2021-0078.
- (28) Li S, Ke Y, Xie L, Zhao Z, Huang X, Wang Y, et al. Study on the aging of three typical rubber materials under high- and lowtemperature cyclic environment. e-Polymers. 2023;23:20208089. doi: 10.1515/epoly-2022-8089.
- (29) Yang L, Dai X, Zhao X, Liu F, Xu Y, Wang Y. Loading conditions impact on the compression fatigue behavior of filled styrene butadiene rubber. e-Polymers. 2023;23:20208091. doi: 10.1515/epoly-2022-8091.
- (30) Lu L, Luo K, Yang W, Zhang S, Wang W, Xu H, et al. Insight into the anti-aging mechanisms of natural phenolic antioxidants in natural rubber composites using a screening strategy based on molecular simulation. RSC Adv. 2020;10:21318-27. doi: 10.1039/d0ra03425h.
- (31) Kong E, Yoon B, Nam J-D, Suhr J. Accelerated aging and lifetime prediction of graphene-reinforced natural rubber composites. Macromol Res. 2018;26:998-1003. doi: 10.1007/s13233-018-
- (32) Lin Y, Yin F, Liu Y, Wang L, Wu K. Influence of vulcanization factors on UV-A resistance of silicone rubber for outdoor insulators. IEEE Trans Dielectr Electr Insulation. 2020;27:296-304. doi: 10.1109/tdei.2019.008483.
- (33) Tjahyono AP, Aw KC, Travas-Sejdic J. A novel polypyrrole and natural rubber based flexible large strain sensor. Sens Actuators B Chem. 2012;166-167:426-37. doi: 10.1016/j.snb. 2012.02.083.
- (34) Zheng T, Zheng X, Zhan S, Zhou J, Liao S. Study on the ozone aging mechanism of Natural Rubber. Polym Degrad Stab. 2021;186:109514. doi: 10.1016/j.polymdegradstab.2021. 109514.
- (35) Xie C, Jia Z, Jia D, Luo Y, You C. The effect of Dy(III) complex with 2-mercaptobenzimidazole on the thermo-oxidation aging behavior of natural rubber vulcanizates. Int J Polym Mater. 2010;59:663-79. doi: 10.1080/00914037.2010.483210.
- (36) Luo Y, Yang C, Chen B, Xu K, Zhong J, Peng Z, et al. Thermal degradation of epoxidized natural rubber in presence of neodymium stearate. J Rare Earths. 2013;31:526-30. doi: 10.1016/ s1002-0721(12)60314-7.

- (37) Komethi M, Othman N, Ismail H, Sasidharan S. Comparative study on natural antioxidant as an aging retardant for natural rubber vulcanizates. J Appl Polym Sci. 2012;124:1490–500. doi: 10.1002/app.35160.
- (38) Simoes RD, Job AE, Chinaglia DL, Zucolotto V, Camargo-Filho JC, Alves N, et al. Structural characterization of blends containing both PVDF and natural rubber latex. J Raman Spectrosc. 2005;36:1118–24. doi: 10.1002/jrs.1416.
- (39) Samran J, Phinyocheep P, Daniel P, Derouet D, Buzaré J-Y. Raman spectroscopic study of non-catalytic hydrogenation of unsaturated rubbers. J Raman Spectrosc. 2004;35:1073–80. doi: 10.1002/jrs.1256.
- (40) Barrera-Garcia VD, Chassagne D, Paulin C, Raya J, Hirschinger J, Voilley A, et al. Interaction Mechanisms between guaiacols and lignin: the conjugated double bond makes the difference. Langmuir. 2011;27:1038–43. doi: 10.1021/ la103810q.
- (41) Li K-J, Wang C, Zheng T-T, Zhao F, Luo M-C, Liao S. Towards high performance anti-aging diolefin elastomers based on structure healing strategy. Polymer. 2020;186:122076. doi: 10.1016/j.polymer.2019.122076.
- (42) Choi S-S, Kim J-C. Lifetime prediction and thermal aging behaviors of SBR and NBR composites using crosslink density

- changes. J Ind Eng Chem. 2012;18:1166–70. doi: 10.1016/j.jiec. 2012.01.011.
- (43) Gan SN, Yahya R, Rooshenass P. Comparison of three different degradation methods to produce liquid epoxidized natural rubber. Rubber Chem Technol. 2016;89:177–98. doi: 10.5254/rct.15.84878.
- (44) Yong MY, Sarih NM, Lee SY, Ang DTC. Biobased epoxy film derived from UV-treated epoxidised natural rubber and tannic acid: Impact on film properties and biodegradability. Reactive Funct Polym. 2020;156:104745. doi: 10.1016/j. reactfunctpolym.2020.104745.
- (45) Zecchini M, Lucas RA, Robertson C, Coban T, Thatti R, Le Gresley A. Investigation of the formation of squalene oligomers exposed to ultraviolet light and changes in the exposed squalene as a potential skin model. Molecules. 2022;27:113481. doi: 10.3390/molecules27113481.
- (46) Yong MY, Ang DTC, Sarih NM. Novel natural rubber-based epoxy coating. Prog Org Coat. 2019;135:105–13. doi: 10.1016/j. porgcoat.2019.05.040.
- (47) Wang X, Fan H, Li W, Zhang Y, Shang R, Yin F, et al. Effect of ultraviolet – A radiation on alicyclic epoxy resin and silicone rubber used for insulators. Polymers. 2022;14:4889–904. doi: 10.3390/polym14224889.